2013 IEEE/RSJ International Conference on
Intelligent Robots and Systems (IROS)
November 3-7, 2013. Tokyo, Japan

Real-time Vision Based Dynamic Sinkage Detection for Exploration Rovers*

Said Al-Milli, Conrad Spiteri, Francisco Comin, and Yang Gao *(Senior Member, IEEE)*

***Abstract*— Identification of the wheel sinkage of exploration rovers provides valuable insight into the characteristics of deformable soils and thus the ease of traversal is also identified. In this paper we propose a simple vision based approach that robustly detects and measures the sinkage of any shaped wheel in real-time and with little sensitivity to various operating conditions. The method is based on color-space segmentation to identify the wheel contour and consequently the depth of the sinkage. In addition, our approach also provides a dynamic sinkage analysis which potentially allows for the identification of non-geometric hazards. The robustness of the algorithm has been validated for poor lighting, blurring, and background noise. The experimental results presented are for a hybrid legged wheel from our in-house single-wheel test-bed.**

I. Introduction

The majority of current planetary exploration rovers are designed with conventional rigid wheels such as MER and MSL. New and emerging research suggests that a faster and more agile breed of scouting rovers are to be used in future exploration missions [1]. These rovers have adopted more complex methods of traversal, e.g. walking, which gives them an extra edge over conventional wheels. A hybrid legged wheel system, such as the one on the Asguard high mobility rover by DFKI (Fig. 1), combines the best of both designs where wheels allow for fast traversal and legs provide the extra agility over highly deformable terrains. As with conventional wheeled rovers, legged rovers would also benefit from identifying the sinkage of their legs to monitor the mobility performance and potentially assess the terrain characteristics.

The sinkage of a wheel can be accurately determined through vision based techniques [6 – 10]. These approaches represent the current state of the art in vision based sinkage detection. In [10] a camera is directed towards a wheel with a pattern of equally spaced 1mm thick concentric black circumferences on a white background. An edge detection algorithm is then employed to identify and count the number of visible radial lines within a region of interest of the sinking wheel to determine the sinkage with high accuracy. It is however unheard of that such solid wheels with radial markings are used in practice. Usually exploration rovers tend to have hollow wheels so as to reduce the weight and minimize soil interaction effects such as bulldozing.

Figure 1. Asguard high mobility rover by DFKI [3]

In [11] the Normalized Cuts method is employed to determine the similarities in pixels' intensity values and their spatial locations. This however is computationally intensive and in order to reduce the computational load the Mean-Shift clustering algorithm is applied to the image as a pre-conditioning stage to obtain homogeneous regions called Super-Pixels. Although this approach seems to produce promising robustness towards poor lighting conditions and shadowing, it remains more computationally intensive than simpler stochastic segmentation approaches.

In [6] the vision based approach uses simple intensity segmentation of a grayscale image to detect the intensity variation between the wheel and the terrain. The beauty of this solution is its simplicity. However, segmentation of grayscale intensity based variations would fail when the contrast between the wheel and the terrain is small and when objects within the Region Of Interest (ROI) of the image frame have similar intensity values to that of the wheel. To improve the efficiency while keeping the approach simple, it was suggested to use color space segmentation in conjunction with a yellow wheel such that the contrast between the wheel and the terrain is kept at a maximum even in poor lighting conditions.

Moreover, the algorithms presented in [6 - 10] are restricted to wheeled vehicles and cannot be adapted for legged or even hybrid legged-wheels as the computation depends on the symmetry of the shape of the wheel at all times and while the wheel rotates. The trajectory of legged or hybrid wheels means that the legs need to be tracked. To our knowledge, there are no vision based techniques that have been developed for measuring or estimating the sinkage for a legged exploration rover. This paper aims to address this by

*Resrach Funded by EU FP7 and in collaboration with the FASTER. www.faster-fp7-space.eu

S. Al-Milli: research fellow and member of the AI and Autonomy Research Group at the Surrey Space Centre, University of Surrey, Guildford, GU2 7XH UK (phone: 0044-1483-682272; fax: 0044-1483-689503; e-mail: s.al-milli@surrey.ac.uk).

C. Spiteri: PhD student at the SSC and is a member of the AI and Autonomy Research Group.

F. Comin: PhD student at the SSC and is sponsored by Becas laCaixa

Y. Gao: Professor in Spacecraft Autonomy and is head of the AI and Autonomy Research Group.

bridging the gap in research for legged exploration rovers towards being realized as formidable alternatives to wheeled rovers. The visual approach presented in this paper is based on detecting the contours of the locomotion system whether it is a wheel or a leg thus making it a generic solution to estimating the sinkage of all kinds of locomotion systems.

The following chapter gives a brief overview of the proposed algorithm. In Chapter III the algorithm is described in further detail and a hybrid legged wheel is used as an example case study. The experimental setup and results are presented in chapter IV and finally the concluding remarks and future steps are presented in chapter V.

II. Algorithm Overview

The vision based sinkage detection algorithm is concerned with measuring the level of sinkage of a wheel into various types of deformable terrain such as soil, sand or loose gravel. In the context of this paper a legged wheel (Fig. 2) is used to determine the efficiency and validity of the algorithm. Since an ordinary wheel has a more straight forward and predictable shape, working with a legged wheel demonstrates the versatility of our algorithm in detecting the sinkage of any locomotion shape.

A camera rigidly mounted below the center of the legged wheel hub, on the belly of the rover, is positioned to "look" at the wheel leg from the moment it touches the terrain to the instance it disconnects (Fig. 2). The maximum level of sinkage is assumed to be half way up the leg; hence the camera FOV needs to cover the whole transition of each leg.

The algorithm is dependent on correctly segmenting the contour of the wheel or leg from the background and from deformable terrain. This is achieved by constructing a wheel using a blue material (Fig. 2) and performing color space segmentation of the wheel. Additionally, an encoder is required to compute the pose of the wheel or leg such that anything that lies outside the ROI is masked. Finally, the sinkage is calculated by measuring the level of occlusion on the leg by the deformable terrain.

The algorithm is constructed using the following steps: A) Image capture and masking, B) Segmentation and morphological operations, C) Detection of wheel contour and interface, D) Calculation of sinkage. These steps are explained in further detail in the following section.

III. Detailed Algorithm Description

The algorithm is only concerned with the 2 dimensional aspect of the wheeled leg since the camera frame is rigidly attached to the wheel frame and therefore the transition of the leg through the image is known at all times.

A. Image Capture and Masking

Images are captured from the camera at the highest possible frame rate. The frame rate is dependent on the processing power and computational resources, however, sub-second measurements are required to ensure real-time performance. The mask consists of 2 polygons and 2 ellipses that create an annular sector which represents a window corresponding to the position of a leg. The ellipses are of a fixed and constant radius so in actual fact they are circles that mark the inner and outermost sections of the annular sector of interest.

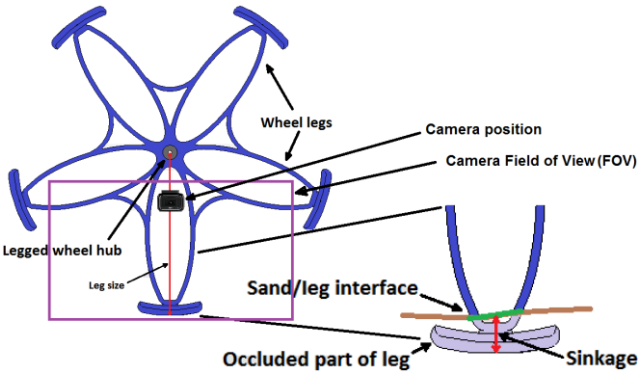

Figure 2. Legged Wheel sinking into deformable terrain

The polygons are computed through simple trigonometry to create an annular sector window through which the leg transitions or, in the case of a circular wheel, the sector that will interact with the deformable terrain. In the case of a circular wheel, a fixed angular sector mask is created that reveals only the sector of the wheel that will interact with the deformable terrain [6]. The part of the image that isn't masked is set as the region of interest where subsequent computations are performed thus having the benefit of reduced noise and increased computation speeds.

B. Segmentation and Morphological Operations

Most color based segmentation techniques are based on the notions of grey-scale methods [7]. The image is transformed into various color spaces and each channel or combination of channels are analyzed as if they were a grey-scale image, then merging the results to obtain a single template that represents the segmented region(s) of interest.

In the context of this paper a simple linear equation is used for color based segmentation to identify blue pixels within the image. The equation assumes that the blue channel value of a pixel that is above a predefined threshold should have a value of at least 40% greater than the red channel within that pixel and should be at least 40% greater than the mean value of the red and green channels within that pixel. This is also described in the following:

$$dst_{(x,y)} = \begin{cases} 0 & if\ (src^{r}_{(x,y)}) \times 1.4 > src^{b}_{(x,y)} \\ 0 & if\ (src^{r}_{(x,y)} + src^{g}_{(x,y)}) \times 1.4 > src^{b}_{(x,y)} \times 2, \\ 0 & if\ src^{b}_{(x,y)}) > thresh \\ 255 & otherwise \end{cases} \quad (1)$$

where *dst* is the output binary image, *src* is the source image captured from the camera, *r*, *g* and *b* are the red, green and blue channels of *src*, *x* and *y* are the pixel row and column within the image and *thresh* is a default threshold value which can be determined by a calibration process at regular intervals or other triggers. Equation 1 can be thought of as an adaptation of the RGB transformation into *rg*-chromaticity with a combined thresholding and segmentation function.

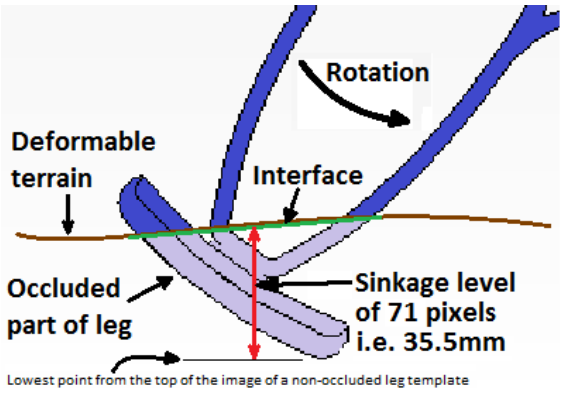

Figure 3. Identification of sinkage from occlusion of locomotion contour

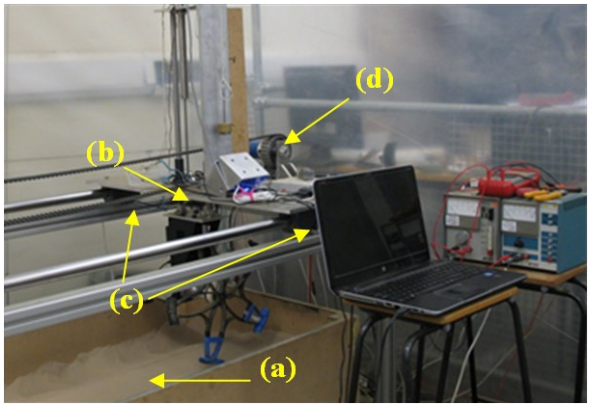

Figure 4. Single Wheel-Leg Test Bed setup: (a) regolith filled rig, (b) moving carriage, (c) translation linear bearings, (d) motor and timing belt

The output of the color based segmentation algorithm is therefore a binary image where pixels with a non-zero value represent the leg in view. The pixels are expected to be in a cluster forming a blob where morphological operators (closing method) are applied to reduce noise.

C. Detection of Contour and Interface

The binary output of the color based segmentation will still occasionally contain noise in the form of sparse clusters of pixels or blobs. There is consequently a necessity to analyze the blobs, eliminate any false positives and detect/analyze the correct blob for sinkage estimation in subsequent steps.

Several different methods that extract object features for comparison and analysis exist and many of which revolve around the geometric properties of low-order moments [8]. In the context of this paper, only basic analysis is required since this function is essentially used as an outlier rejection mechanism. Therefore a comparison of the blob's Zeroth Moment (*i.e.* the area), is preformed where the largest value is assumed to be the object of interest. The general equation of a moment is:

$$M = \sum_{r=1}^{R}\sum_{c=1}^{C} r^i c^j I(r,c), \qquad (2)$$

where R is the number of Rows, C the number of columns and $I(r,c)$ for a binary image is ϵ [0,1] $\forall$ r,c. Therefore the zeroth order moment A (area) of a binary image can be computed by:

$$A = \sum_{r=1}^{R}\sum_{c=1}^{C} I(r,c). \qquad (3)$$

The contour of the largest blob is then extracted using a border following method as described by Suzuki [9].

Since the camera field of view and the aperture of the region of interest are quite narrow, the deformable terrain is not expected to have much height and depth variations within this area. It is therefore safe to assume that the deformable terrain is roughly flat at the ROI. The interface between the sand and the wheel is determined by the distance of each contour point from the top of the image. The furthest 3% of contour pixels from the top of the image are considered to be the interface or the extremities of the leg.

D. Sinkage Determination

The sinkage is calculated by measuring the level of occlusion on the leg caused by the deformable terrain. Since the camera frame and the wheel frame are rigidly attached while in the case of a legged wheel, the angle of each leg is known from the wheel encoder, the sinkage calculation becomes is a simple template subtraction.

The actual sinkage is a comparison between the lowest point from the top of the image of a non-occluded leg template at a given angle of rotation and the lowest point from the top of the image of an occluded leg at the same angle (Fig. 3).

IV. Experimental Results

Tests were carried out in a Single Wheel-Leg Test Bed (SWLTB) to evaluate the performance of the proposed vision-based sinkage algorithm and to validate the sinkage detection produced.

A. Apparatus Description

The SWLTB setup and its main components are shown in Fig. 4. It consists of a wooden rectangular rig (a), where granular regolith is contained, and an aluminum frame that supports a moving carriage (b). Translation of the carriage is attained by means of two linear bearings (c), a motor and a timing belt (d).

The wheel-leg, its motor and the related sensors are fixed to a support structure, shown in Fig. 5. The structure sinks freely thanks to two linear bearings (a). A linear position transducer (b) measures vertical displacement of the wheel-leg relative to the carriage and a pulley permits applying counterbalance normal loads using dead weights (c). An absolute angular encoder on the output shaft of the wheel-leg motor (d) provides measurements of the angular position of the wheel-leg with 0.1 degrees of resolution. A USB camera (e) is mounted on the structure so that the area where the legs sink into the regolith is centered inside its field of view.

B. Experimental Preparation and Procedure

Two of the legs of the wheel-leg, shown in Fig. 6, are wrapped with blue tape up to a 75mm sinkage level and a

1mm black and white stripe ruler was attached for manual sinkage validation. Special feet were manufactured in blue material for both legs. For the tests, a Martian regolith simulant available at Surrey Space Centre (SSC-2) is used in the experiments. The regolith consists of fine Garnet sand, with particle sizes ranging from 45 to 90 µm.

Before every test the regolith is raked to homogenize it and regenerate disturbed soil, maintaining a consistent configuration throughout all the tests. The soil is then leveled in order to maintain a constant height within the millimeter for the signal from the sinkage transducer to be reliable. During the tests, a microcontroller takes readings from the wheel-leg encoder and the carriage sinkage transducer. A C++ script running on a laptop queries these values from the microcontroller, captures images from the USB camera and synchronizes the data with a millisecond timestamp.

C. *Experimental Configurations*

Experiments were carried out using the SWLTB to test for three main factors that make vision based algorithms fail. These factors are namely: poor lighting, blurring, and background noise. In our case, background noise is described as objects within the ROI that could interfere with our predictions such as rocks or shadows. A total of four experiments were conducted where the normal load on the wheel was 3.5kg for one pair of experiments and 1kg for the other pair. In each pair an experiment was conducted with normal laboratory lighting conditions and the other with poor lighting conditions. The luminance of normal lighting was measured to be between 300-400 Lux within the test-bed whereas the luminance was varying between 10-50 Lux for poor lighting. In all four experiments dark rocks were laid out behind the wheel's path. Figures 8, 9, and 10 show processed images from various stages of the algorithm including (1) the input image with the detected interface line overlaid, (2) the color segmented binary image, (3) the masked binary image and (4) the ROI of the input image.

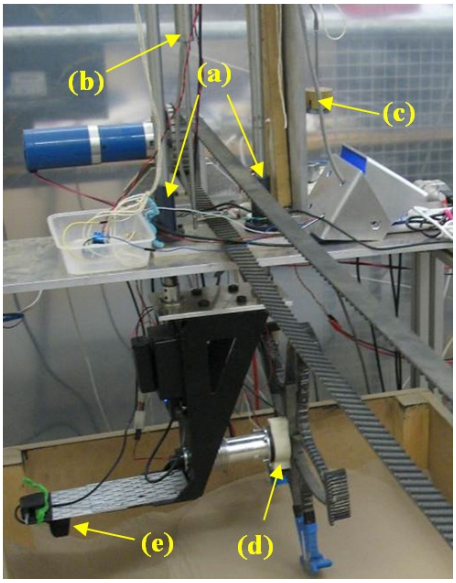

Figure 5. Wheel-leg support structure: (a) sinkage linear bearings, (b) linear transducer, (c) counterbalance normal loads, (d) motor output shaft absolute encoder, (e) USB camera

The normal laboratory lighting conditions seen in Fig. 8 demonstrate that the algorithm is capable of filtering interfering background objects with similar intensity contrast to the leg. Likewise the detection is accurately demonstrated in poor lighting conditions even though such conditions have caused a tint of blue into the majority of the image frame as seen in Fig. 9(2). And although the blue tinged pixels are picked up by the algorithm they are filtered out as the algorithm selects only the largest blob in the ROI. Finally Fig. 10 demonstrates the detection in a scenario where all the performance impacting factors exist including blurring.

Figures 11-14 are the product of processing the image sequences of all four experiments and comparing the sinkage detections with the measured leg sinkage from the linear position transducer where L1 and L2 denote data of the first and second blue legs in the sequence. Generally, the trend of the algorithm predictions is in good agreement with our measured ground truths and our detected rate of sinkage also follows that of the measured data. There exists a pair of deflection points while the leg sinks into the sand and another when the leg exits. This is due to minor friction exhibited from the linear bearings Fig. 6(a) which is picked up by the position transducer. This is equally demonstrated from our algorithms' detections. Also note that the first leg sinks less into the sand than the second due to the friction within the linear bearings. Detection of such sudden changes in sinkage rates is gaining substantial interest in the planetary exploration community which allows the identification of non-geometric hazards such as duricrust formations over highly deformable terrains. This phenomenon is what has caused the MER rover Spirit to become entrenched in late 2009.

The detection errors attributed to the conducted experiments are presented in Table 1. Since the detected sinkage fluctuates, 5-point centered moving averages were computed to smooth the data and used to compute the average errors. Peak errors are ones where the difference between the moving average detections and ground truth measurements are highest for a particular time stamp. It is clear from the errors that the algorithm's accuracy is rather high even though some of the operational conditions at which the detections took place were far from ideal (10-50 Lux) given that planetary rovers in Mars only operate during mid-day (300+ Lux). In fact the highest average error of

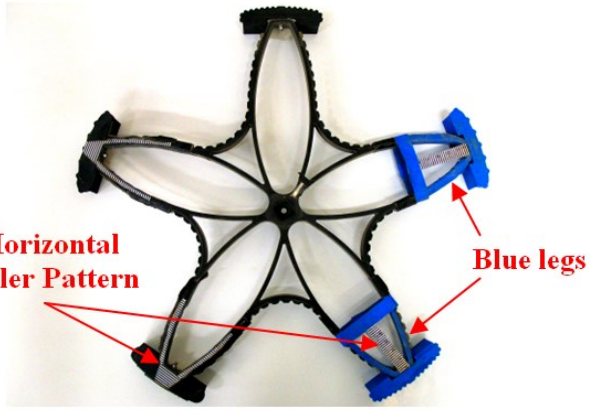

Figure 6. Asguard Wheel-Leg from DFKI [3] with blue legs and feet

22.1% was detected for the first blue leg during poor lighting conditions due to the leg being further away from the light source than the second leg (see Fig. 14) and thus close to the cameras' minimum operating luminosity of around 10Lux. As the wheel moved closer to the light source the sinkage of the second leg was detected with an average accuracy of 7.4%

E. Computational Performance

The algorithm was implemented in C++ and utilizes the OpenCV library to ensure that the performance is optimized. The algorithm was run on a virtual machine Linux distribution with a single 2GHz[1] virtual CPU core and 512Mb of virtual RAM. The CPU time of the virtual core was throttled down to simulate various CPU speeds as found on On-Board Computers (OBC) of explorations rovers. The speeds are: 200MHz, 500Mhz, 700Mhz, 1Ghz, and 2Ghz and the corresponding frame rate of our algorithm is shown in Fig. 7. It is worth noting that the MER rovers had an OBC with 200MHz and that the Raspberry Pi (an inexpensive computer) has a CPU speed of 700Mhz, both of which would be capable of dynamically assessing the sinkage with our proposed algorithm.

V. CONCLUSION

A generic vision based sinkage detection solution for detecting the sinkage of any type of locomotion systems of exploration rovers has been presented. Color space segmentation is used on a ROI within the image frame and the largest blob is selected for sinkage analysis. Experimental results show the robustness of successful detections even in noisy and blurry situations or even in poor lighting conditions. The performance of the algorithm was tested for

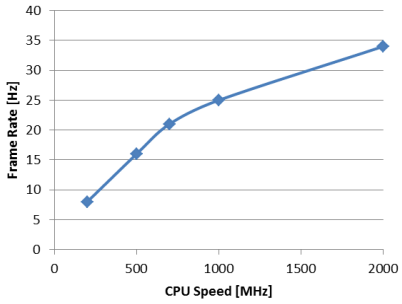

Figure 7. Algorithm frame rate for various CPU speeds

TABLE I. VISION BASED DETECTION ERROR (% OF GROUND TRUTH)

Exp No.	Leg 1. Error		Leg 2. Error	
	Avr [%]	Max [%]	Avr [%]	Max [%]
1.	6.7	19.6	5.9	22.1
2.	9.3	34.4	6.9	27.9
3.	9.0	21.0	9.5	33.8
4.	22.1	55.5	7.4	19.9

Table 1. Avr = 5-point centered moving averages. Max = max difference between moving average detections & ground-truth measurements.

[1] The host computer was a Dell XPS with an Intel Core i7-2630QM CPU @ 2.00GHz.

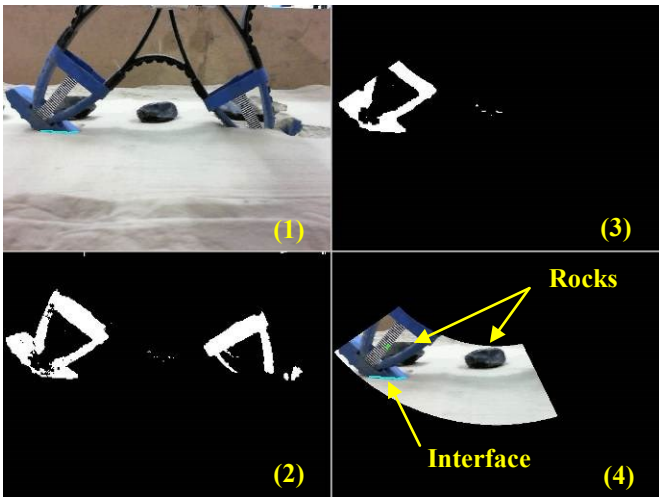

Figure 8. Processed image from the proposed vision based Algorithm for the normal operating conditions scinario. The luminance value was between 300-400 Lux.

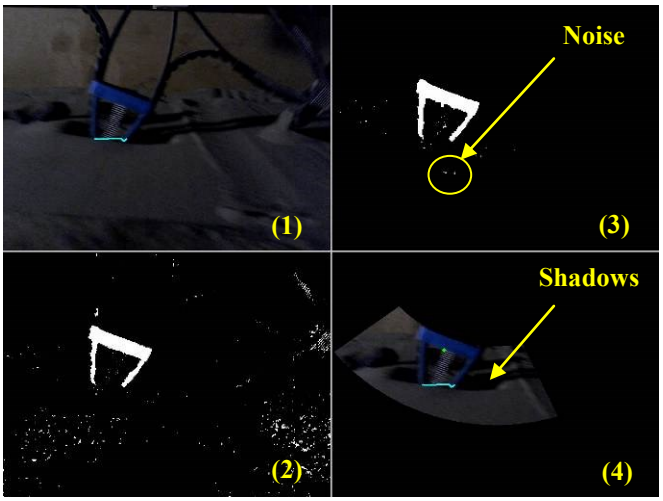

Figure 9. Processed image from the proposed vision based Algorithm for the poor lighting conditions scinario. Luminance = 10-50 Lux.

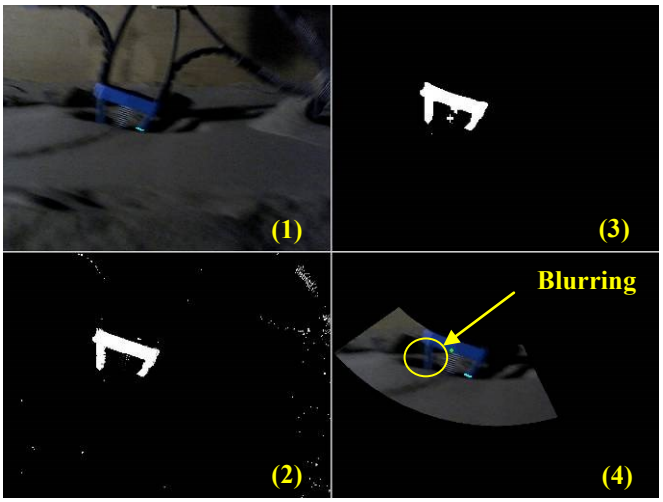

Figure 10. Processed image from the proposed vision based Algorithm for the poor lighting conditions and blurring scinario. Luminance = 10-50 Lux.

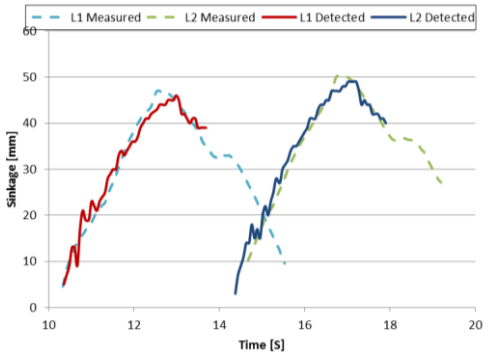

Figure 11. Exp.1 - Measured and Detected leg sinkage. Normal load = 3.5kg, luminance = 300-400 Lux, and wheel speed = 7cm/s

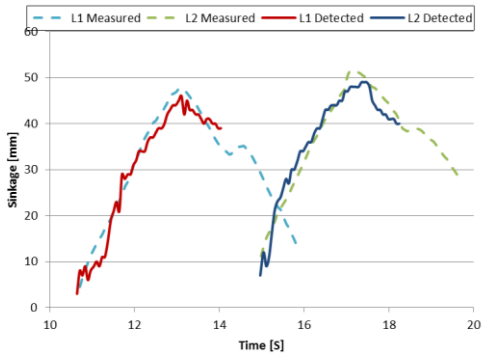

Figure 12. Exp.2 - Measured and predicted leg sinkage. Normal load = 3.5kg, luminance = 10-50 Lux, and wheel speed = 7cm/s

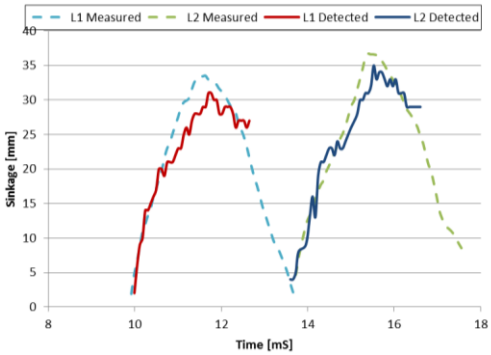

Figure 13. Exp.3 - Measured and predicted leg sinkage. Normal load = 1.0kg, luminance = 300-400 Lux, and wheel speed = 7cm/s

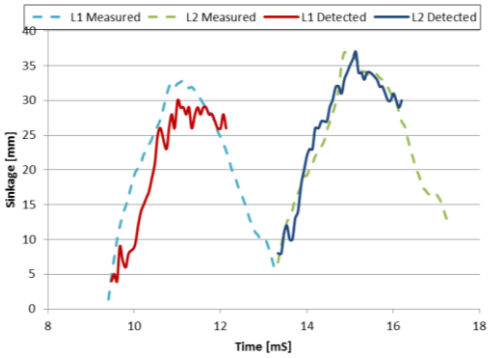

Figure 14. Exp.4 - Measured and predicted leg sinkage. Normal load = 1.0kg, luminance = 10-50 Lux, and wheel speed = 7cm/s

various CPU speeds to demonstrate its ability to dynamically assess sinkages. Finally the algorithm achieves a high level of accuracy when the luminance level is higher than 10Lux which is usually the case for exploration rovers as they are dependent on solar power.

Future work will focus on further improving the accuracy through template matching and subtraction as well as introducing a dynamic masking algorithm which would allow for a tighter ROI that moves along with the wheel/leg this would also mean that the detection range of the sinking leg would increase and that the sinkage detection of two simultaneously sinking legs would also be possible.

ACKNOWLEDGMENT

This research is funded by EU Framework Programme call No. 7. We also would like to thank DFKI for providing us with their high mobility legged-wheel and Chris Brunskill for developing the Single Wheel Test Bed at SSC.

REFERENCES

[1] S. Colombano, F. Kirchner, D. Spenneberg, J. Hanratty, “Exploration of Planetary Terrains with a Legged Robot as a Scout Adjunct to a Rover,” American Institute of Aeronautics and Astronautics, Space 2004 Conference, San Diego, California (2004)

[2] M. Eich, F. Grimminger, S. Bosse, D. Spenneberg, F. Kirchner, “Asguard: A Hybrid -Wheel Security and SAR-Robot Using Bio-Inspired Locomotion for Rough,Terrain” International Workshop on Robotics for Risky Interventions & Surveillance of Environment, Benicàssim Spain 2008

[3] Eich, M., Grimminger, F., Kirchner, F. A versatile stair-climbing robot for search and rescue applications. Proceedings of the 2008 IEEE, International Workshop on Safety, Security & Rescue Robotics, Sendai, Japan 2008.

[4] J. Schwendner, F. Grimminger, S. Bartsch, T. Kaupisch, M. Yuksel, A Bresser, J. B. Akpo, M. K.-G. Seydel, A. Dieterle, S. Schmidt and F. Kirchner, “CESAR: A Lunar Crater Exploration and Sample Return Robot,” IEEE/RSJ International Conference on Intelligent Robots and Systems, October 11-15, 2009 St. Louis, USA

[5] S. Colombano, F. Kirchner, D. Spenneberg, J. Hanratty, “Exploration of Planetary Terrains with a Legged Robot as a Scout Adjunct to a Rover”, American Institute of Aeronautics and Astronautics, Space 2004 Conference, San Diego, California. 2004.

[6] Christopher A. Brooks, Karl D. Iagnemma, and Steven Dubowsky, “Visual wheel sinkage measurement for planetary rover mobility characterization,” Auton. Robots, Vol. 21, No. 1, pp. 55-64, August 2006

[7] Kanchan Subhash Deshmukh, “Color Image Segmentation: A Review”, Second International Conference on Digital Image Processing, Proc. of SPIE

[8] R.J. Prokop, A.P. Reeves , “A Survey of Moment-Based Techniques for Unoccluded Object Representation and Recognition”, CVGIP: Volume 54, Issue 5, September 1992, Pages 438–460

[9] Satoshi Suzuki, “Topological Structural Analysis of Digitized Binary Images by Border Following”, Computer Vision, Graphics and Image Processing, N 32-46 1985.

[10] G. Reina, L. Ojeda, A. Milella, and J. Borenstein, “Wheel Slippage and Sinkage Detection for Planetary Rovers,” IEEE/ASME Transactions on Mechatronics, Vol. 11, No. 2, April 2006

[11] G.-P. Hegde, C.J. Robinson, Ye Cang, A. Stroupe, and E. Tunstel, “Computer vision based wheel sinkage detection for robotic lunar exploration tasks,” Mechatronics and Automation (ICMA), 2010 International Conference on , vol., no., pp.1777-1782, 4-7 Aug. 2010

[12] Dario L. Sancho-Pradel and Yang Gao, “A Survey on Terrain Assessment Techniques for Autonomous Operation of Planetary Robots”, Journal of British Interplanetary Society, Vol. 63, No. 5/6, pp. 206-217, May/June, 2010